Indian Journal of Advances in Chemical Science

Article

Dual Responsive Aminothiazole based Antibacterial Copolymeric Nanogels for Controlled Release of Anti-Human Immunodeficiency Virus Drug Zidovudine

Sana Eswaramma[1], Kummara Madhusudana Rao[2], G. Viswanatha Reddy[3], K. S. V. Krishna Rao[1]*

[1]Polymer Biomaterial Design and Synthesis Laboratory, Department of Chemistry, Yogivemana University, Kadapa, Andhra Pradesh, India, [2]School of Chemical Engineering, Yeungnam University, Gyeongsan, South Korea, [3]Department of Chemistry, Rajiv Gandhi University of Knowledge Technologies, Vempalli, Andhra Pradesh, India

ABSTRACT

Dual responsive copolymeric poly(*N*-(2-aminothiazolyl) maleamic acid-co-*N*-isopropyl acrylamide) nanogels (PAMNI-NGs) produced from *N*-(2-aminothiazolyl) maleamic acid (AMA) and *N*-isopropyl acrylamide (NIPAM) through a simple free radical emulsion polymerization. The formations of PAMNI-NGs were confirmed by Fourier-transform-infrared (FTIR) spectroscopy, dynamic light scattering (DLS), transmission electron microscopy (TEM), and atomic force microscopy (AFM). TEM and DLS results gave the surface morphology and particle size, respectively, that PAMNI-NGs are semi slightly spherical and are found around 100 nm, further it is confirmed with AFM. Further, Zidovudine (ZDV), an anti-human immunodeficiency virus drug, was successfully loaded into the developed PAMNI-NGs using an equilibrium swelling method. The formation of PAMNI-NGs was investigated through FTIR, DLS, AFM, and transmission electron microscopy (TEM) analyses, while the ZDV-loaded PAMNI-NGs were confirmed from FTIR and XRD studies. The encapsulation efficiency of ZDV is varied from 33 to 82%. The *in vitro* release studies of ZDV from the PAMNI-NGs were examined in different gastrointestinal tract pH conditions (pH 1.2 and 7.4) at 25° and 37°C. The presence of aminothiazole functionality in the PAMNI-NGs also showed excellent antibacterial activity towards bacterial strains of Gram-positive (*Bacillus cereus* and *Staphylococcus aureus*) and Gram-negative (*Escherichia coli* and *Klebsiella pneumoniae*).Therefore, the *in vitro* release and antibacterial studies revealed the efficiency of PAMNI-NGs toward site specific drug delivery and antimicrobial applications, respectively.

Key words: N-(2-aminothiazolyl) maleamic acid, *N*-isopropyl acrylamide, Copolymer, Nanogels, Controlled release, Antibacterial activity.

1. INTRODUCTION

Nanotechnology is an emerging field in medicine that has been introduced new opportunities for medical care by achieving significant therapeutic benefits [1]. Since past 30 years, a wide variety of nanocarriers has been proposed for biomedical fields especially in drug delivery. Different nanocarriers have been designed and developed for pharmaceutical applications due to their tunable physicochemical properties and mechanical stability. Among those nanocarriers, liposomes, nanospheres, nanogels, dendrimers, and quantum dots are recently well investigated. Of those different kinds of polymeric nanocarriers, a specific consideration has been deserved for nanogels (NGs) [2,3]. NGs are nanoscale polymer hydrogel networks which offer favorable physicochemical characteristics including narrow size distribution (50–400 nm), huge tendency to imbibe water, superior colloidal stability, and high surface to volume ratio [4]. In the literature, various polymeric NGs were reported for a wide range of biomedical applications [1]. However, a significant challenge has been faced in the pharmaceutical drug delivery due to the lack of optimal therapeutic activity of drugs led to cause adverse side effects. Therefore, NGs have come into the field over conventional macromolecular devices. The advantageous properties of NGs such as high stability, ease of synthesis, high entrapment efficiency, significant responsive behavior, and good control over particle size, which allow them as ideal candidates for pharmaceutical treatment of wide range of diseases including cancer, acquired immunodeficiency syndrome (AIDS) [5,6], and delivery of proteins and genes [7,8].

Thiazoles and their derivatives are that the important class of biologically active molecules has been found many potential applications in pharmaceutical and biomedical areas. The biological activity of thiazoles is mainly aroused from their diverse chemical structures which allow a broad range of applications during the development of drugs for the treatment of cancer, allergies, tuberculosis, hypertension, inflammation, and human immunodeficiency virus (HIV) infections [9,10]. Recently, the aminothiazoles are also acted as ligands for estrogen receptors as well as adenosine receptor antagonists [11]. Another class of thiazole derivatives exhibits anti-mycobacterial and anti-plasmodial activity and has been exploited in the development of anti-mycobacterial and anti-plasmodial drugs [12]. A novel class of thiazoles and fused thiazole derivatives possess anticancer activity,

***Corresponding author:**
K. S. V. Krishna Rao
E-mail: ksvkr@yogivemanauniversity.ac.in

ISSN NO: 2320-0898 (p); 2320-0928 (e)
DOI: 10.22607/IJACS.2022.1002004

Received: 26th February 2022;
Revised: 10th March 2022;
Accepted: 21st March 2022

whereby they act on cancer biotargets including tumor necrosis factor TNF-α, inosine monophosphate dehydrogenase, and apoptosis inducers [13]. 2-amino thiazoles and their analogs potentially interact with DNA minor groove; hence, the template function of DNA blocked. In this way, the amino thiazoles and their structurally related compounds have shown good antitumor activity through DNA binding properties [14]. Due to its antibacterial activity, 2-amino thiazole can also be used in the treatment of hyperthyroidism [15]. The anti-parasitic spectrum of 2-amino thiazoles has also been investigated and reported in the literature [16]. The presence of N atom in the thiazole moiety provides excellent binding behavior to thiazole analogs for metal ions and biological molecules [9,17].

It is well known that poly(N-isopropyl acrylamide) (PNIPAM) is a well investigated, thermosensitive polymer exhibits lower critical solution temperature (LCST) around 32–34°C in aqueous solution [18]. The thermosensitive hydrogels exhibit typical volume phase transition behavior at their LCST, results in the formation of sudden phase transformation from hydrophilicity to hydrophobicity [19]. Due to this phase transition behavior, this kind of thermo sensitive hydrogels could work as on-off triggers for pulsatile controlled release of drugs [20,21]. pH and thermo responsive hydrogels are promising for drug delivery applications. The incorporation of pH sensitive moieties into the thermoresponsive NGs exhibited dual responsive behavior (pH and temperature). Rao *et al.* developed the dual responsive NGs by incorporation of glycolic acid units into thermoresponsive polymer NGs and used for controlled drug delivery 5-flurouracil [22]. In the present study, 2-amino thiazole was modified into its acid derivative, N-(2-aminothiazolyl)maleamic acid (AMA) that has shown excellent pH-sensitivity under physiological pH conditions [17]. Further, the NGs were prepared using modified pH sensitive AMA and temperature responsive NIPAM monomers for both controlled release and antibacterial applications. The incorporation of pH sensitive AMA monomer into thermoresponsive polymer network not only provide the dual responsive property but also beneficial for their excellent antibacterial activity.

An anti-HIV drug, zidovudine (ZDV), a nucleoside reverse transcriptase inhibitor, has approved and been used in the treatment of AIDS/HIV infection [23]. However, the therapeutic efficacy of ZDV is seriously limited due to its poor availability (60%), short biological half-life (1–3 h), dose dependent hematological toxicity, and reduced therapeutic index [24,25]. To provide an effective therapeutic treatment for AIDS, it is necessary to maintain the systemic concentration of anti-retroviral drugs in its plasma levels, which can be achieved by developing potential controlled release devices for ZDV. Herein, the present study formulated ZDV-loaded poly(*N*-(2-aminothiazolyl) maleamic acid-co-*N*-isopropyl acrylamide) nanogels (PAMNI-NGs) result in reproducible drug absorption and reduced dosage frequency which can improve the patient compliance compared to burst release dosage forms [25,26].

2. MATERIALS AND METHODS

2.1. Materials

N-isopropyl acrylamide (NIPAM) was purchased from Sigma Aldrich Co. *N,N'*-methylene bis-acrylamide (MBA) and sodium dodecyl sulfate was purchased from S.D. fine Chemicals, Mumbai, India. Ammonium persulfate (APS) was purchased from Merck, Mumbai, India. ZDV, purity >97% was received from the Samchully Pharmaceutical Company, Seoul, South Korea, purchased from *N*-(2-aminothiazolyl) maleamic acid (AMA), was synthesized as per earlier procedure published in elsewhere [17]. Throughout experiment, double distilled water (DDW) was used.

2.2. Preparation of Poly(AMA-co-NIPAM) (PAMNI) Nanogels

A simple free radical emulsion polymerization was involved in the preparation of poly(AMA-co-NIPAM) NGs, wherein APS, MBA, and SDS were used as free radical initiator, crosslinker, and emulsifying/colloidal stabilizing agent, respectively. At first, AMA monomer was taken in a three necked round bottom flask, and then dissolved in 100 mL of DDW to get clear yellow colored solution. Subsequently, prenoted weights [Table 1] of NIPAM, MBA and APS were added followed by SDS (1.0 g) in to the same flask, which, therefore, fitted with a reflux condenser and a nitrogen inlet. The contents of the flask were gently bubbled with nitrogen gas for 60 min to create an inert atmosphere within the flask. Thereafter, the flask was placed on a heating bath to maintain the temperature around 70°C and the contents were continuously stirred well at 800 rpm for 8 h. After the reaction time was over, the flask containing reaction mixture was taken out from the bath, cooled to room temperature using running tap water. Later, the mixture was poured into calcium chloride solution (5 wt%) under high rotation speed to break the emulsifying medium into NGs, which were collected by centrifugation operated at 15,000 rpm for 30 min. The NGs obtained were immersed in DDW for 5 days to eliminate the traces of monomers, initiator, and crosslinker. Further, the NGs were collected by performing centrifugation again at similar previous conditions. These isolated NGs were dried at room temperature followed by at 40°C using hot air oven and were preserved in a desiccator for further investigations of the present study. The schematic representation of PAMNI copolymeric NGs is shown in Scheme 1. The photographic images of PAMNI copolymeric NGs at two different temperatures (25 and 37°C) were displayed in Figure 1.

2.3. Characterization

Fourier transform infrared (FTIR) spectra of NGs were recorded using Perkin Elmer (Spectrum two model, UK) to verify the formation and interactions of functional groups. The NGs samples were finely grounded with KBr and pellets were prepared under hydrolytic pressure (600 kg/cm^2) and the spectra were recorded in the range 4000–400 cm^{-1}. To ensure the molecular level, distribution of ZDV present in the NGs was assessed using X-ray diffraction patterns and was performed at 2theta of 10–80° using X-ray diffractometer (Rigaku, Japan). Transmission electron microscopy of NGs was performed (TEM TecnaiT-12, Cambridge, England) and operating at an accelerating

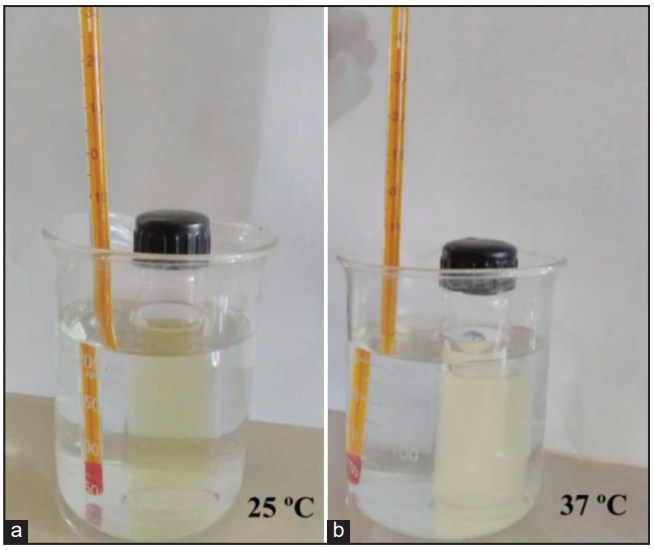

Figure 1: Phase transition behavior of PAMNI nanogels at (a) 25°C and (b) 37°C.

voltage of 200 kV. A droplet of NG suspension was deposited on the copper grid and allowed to dry under the lamp. The morphology and size distribution were analyzed by atomic force microscopy (AFM) and the images were recorded through multimode AFM using NTEGRA PRIMA (NTMDT, Ireland). A drop of the aqueous dispersion of NGs (0.1 mg/mL) was placed on the fresh cleaved mica surface and was air dried at ambient temperature (25°C). The microscopic images were taken by scanning different positions of mica. Dynamic light scattering (DLS) studies were performed to measure the mean diameter and size distribution of NGs using Bruker zetasizer (Model nano-S90, Malvern, UK).

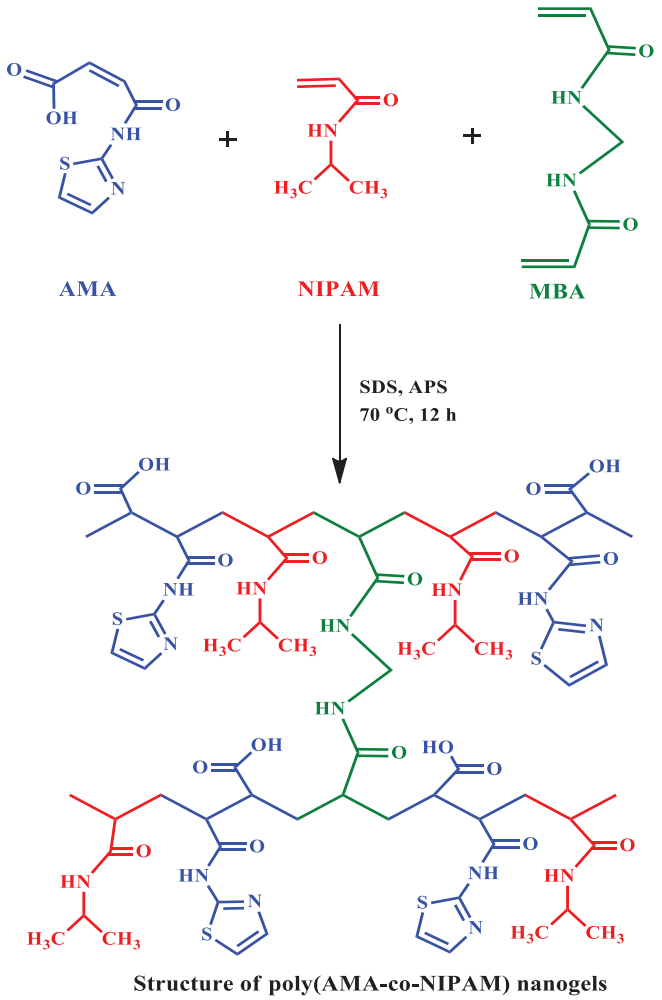

Scheme 1: Schematic representation of PAMNI-NGs.

Table 1: Feed compositions and % encapsulation efficiency of PAMNI-NGs.

Code	AMA (g)	NIPAM (g)	MBA (g)	APS (g)	% EE±S.D
PAMNI-1	0.0	0.5	0.075	0.1	33±0.9
PAMNI-2	0.25	0.5	0.075	0.1	79±1.5
PAMNI-3	0.5	0.5	0.075	0.1	76±1.3
PAMNI-4	1.0	0.5	0.075	0.1	82±1.2
PAMNI-5	0.5	0.0	0.075	0.1	78±0.6
PAMNI-6	0.5	1.0	0.075	0.1	64±1.0
PAMNI-7	0.5	0.5	0.025	0.1	82±0.8
PAMNI-8	0.5	0.5	0.125	0.1	51±1.2

2.4. Drug Loading and Encapsulation Efficiency

ZDV loaded NGs were prepared by equilibrium swelling of PAMNI-NGs (50 mg) in known concentration of ZDV solutions (25 mg/mL). During the swelling of PAMNI-NGs, maximum ZDV was loaded. Thereafter, the ZDV-loaded NGs were filtered from the solution. The initial ZDV solutions and filtrate remaining ZDV solutions were then analyzed to determine the ZDV in PAMNI-NGs using UV-Vis spectrophotometer (UV-3092, LAB INDIA) at a λ_{max} of 269 nm. The experimental values obtained through these studies were used to calculate the % drug loading and % encapsulation efficiency by the following equations.

$$\% \text{ Drug loading} = \left(\frac{\text{Amount of drug in hydrogels}}{\text{Amount of hydrogels}} \right)$$

$$\% \text{ Encapsulation efficiency of ZDV} = \left(\frac{\text{Actual drug loading}}{\text{Theoritical loading}} \right) \times 100$$

2.5. In Vitro Release Studies

To verify the release profiles of encapsulated ZDV from the NGs, the *in vitro* release studies were performed in both simulated gastric (pH 1.2) and phosphate buffer saline (pH 7.4) using Tablet Dissolution Tester Apparatus (DS-8000, LABORATORY INDIA, India). Approximately 100 mg of drug loaded samples were evaluated for release studies by placing each sample into an individual basket containing 500 mL of release medium, maintained at 37±0.5°C with the rotation speed of 100 rpm. At predetermined regular time intervals, 5 mL of release medium was taken from each basket and was used to analyze the amount of drug spectrophotometrically, using UV-Vis spectrophotometer (UV-3092, LABORATORY INDIA, Mumbai, India) by measuring the absorbance of the sample aliquots at a wavelength of 269 nm. The release studies were performed in triplicate for standard deviation.

To understand the ZDV release kinetics of ZDV loaded NGs, the release data were fitted by following various empirical kinetic models [27].

- Zero order equation: $Q=Q_0-K_0\,t$
- First order equation: $lnQ=lnQ_0-K_1t$
- Hixson-Crowell cube root equation: $Q^{1/3}=Q_0^{1/3}\,K_C\,t$.

Where, Q and Q_0 are the amounts of ZDV at time t and at t=0, $K0$, $K1$, and K_C are the rate constant for zero order, First order and Hixson-Crowell cube root law equations, respectively.

Higuchi square root equation: $M_t=K_H^{1/2}\,t$

Koresmeyer-Peppas kinetic equation: $\frac{M_t}{M_\infty} = K_p t^n$

Where, M_t and M_∞ represent the amount of ZDV released by the nanogel at time t and at equilibrium, K_H, and K_p are the rate constant for Higuchi square root and Koresmeyer-Peppas kinetic equations, respectively.

2.6. Antibacterial Studies

The antibacterial activity was screened out for developed copolymeric PAMNI-NGs using disc diffusion method and by evaluating the zone of inhibition [27]. The antibacterial activity of the PAMNI-NGs was tested against both Gram-negative (*Escherichia coli* and *Klebsiella pneumonia*) and Gram-positive (*Bacillus cereus* and *Staphylococcus aureus)* bacteria. The inoculum of the bacterial culture (100 µL) was distributed uniformlyon the agar media plates using a sterile spreader

as per previously reported procedure. The sterile paper discs (6 mm diameter) containing nanogels (30 µL of nanogel suspensions [1 mg/mL]) were used to place on to the surface of inoculated agar plates. The plates were incubated at 37°C for 12 h. Finally, the plates were examined to measure the zone of inhibition around the disc (in mm). The antibiotic drug was used as control.

3. RESULTS AND DISCUSSION

3.1. FTIR Analysis

The synthesized monomer AMA was characterized earlier by our research group [17]. FTIR spectra of placebo NGs [Figure 2a] showed characteristic absorption band at 3418 cm^{-1}corresponds to –NH and –OH stretching vibrations of amine and acid groups, respectively. The bands appeared at 3189 and 2922 cm^{-1} belong to C-H stretching of thiazole ring and aliphatic chain of the network. The C=O stretching vibration of acid and amide is included in the strong band observed at 1680 cm^{-1}. Additional characteristic absorption bands appeared at 1606, 1451, 1399, and 1354 cm^{-1} are due to C=C stretching of thiazole ring, C-H bending, O-H bending of carboxylic acid, and C-N stretching, respectively. The vibrational band at 1226 cm^{-1} was found for C-S stretching of thiazole moiety. All these characteristic vibrational bands confirmed the presence of functional groups in the structure of the NG network. On the other hand, the FTIR spectra of pristine ZDV [Figure 2c] showed that its very intense characteristic absorption bands at 3465, 2079, and 1679 cm^{-1} are assigned to N-H, azide, and carbonyl stretching vibrations of ZDV. These prominent bands of ZDV were also found in the ZDV encapsulated NGs [Figure 2b], confirmed the presence of traces of the drug in the NG network through physical interactions only.

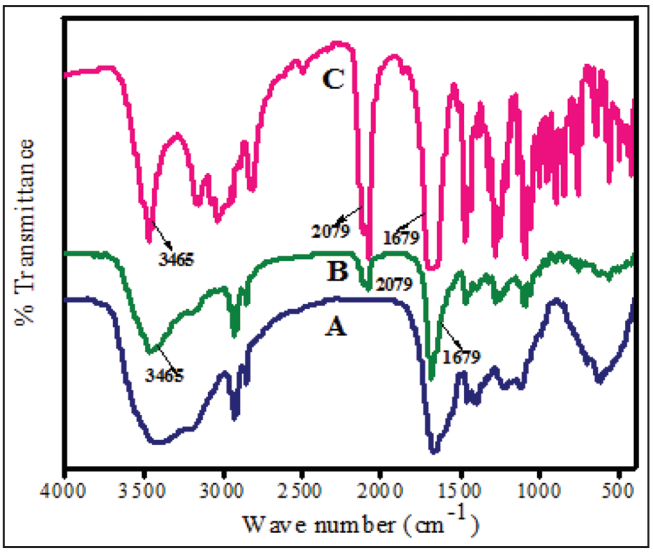

Figure 2: FTIR spectra of (a) placebo PAMNI-NGs, (b) ZDV-loaded PAMNI-NGs, and (c) pristine ZDV.

3.2. Size and Morphological Study

DLS studies were performed to analyze the size of NGs and the size distribution curves of PAMNI-2, PAMNI-3, and PAMNI-4 are shown in Figure 3. The aqueous dispersions of NGs exhibit unimodel size distributions with maximum intensity at 113 nm could suggest good control over particle size. On the other hand, the particle size varied with AMA monomer, the increase in the AMA content also increased the particle size due to insufficient surfactant availability to cover overall the surface of NGs. Thus, the larger particle size results resulted from the coalescence of NGs during the polymerization process.

The surface morphology of PAMNI-2-NGs was next confirmed from AFM studies by magnifying a specific small region of the NG surface using tapping mode and the corresponding figure is shown in Figure 4a and b. In the figure, the brighter spots indicate the more rigid component

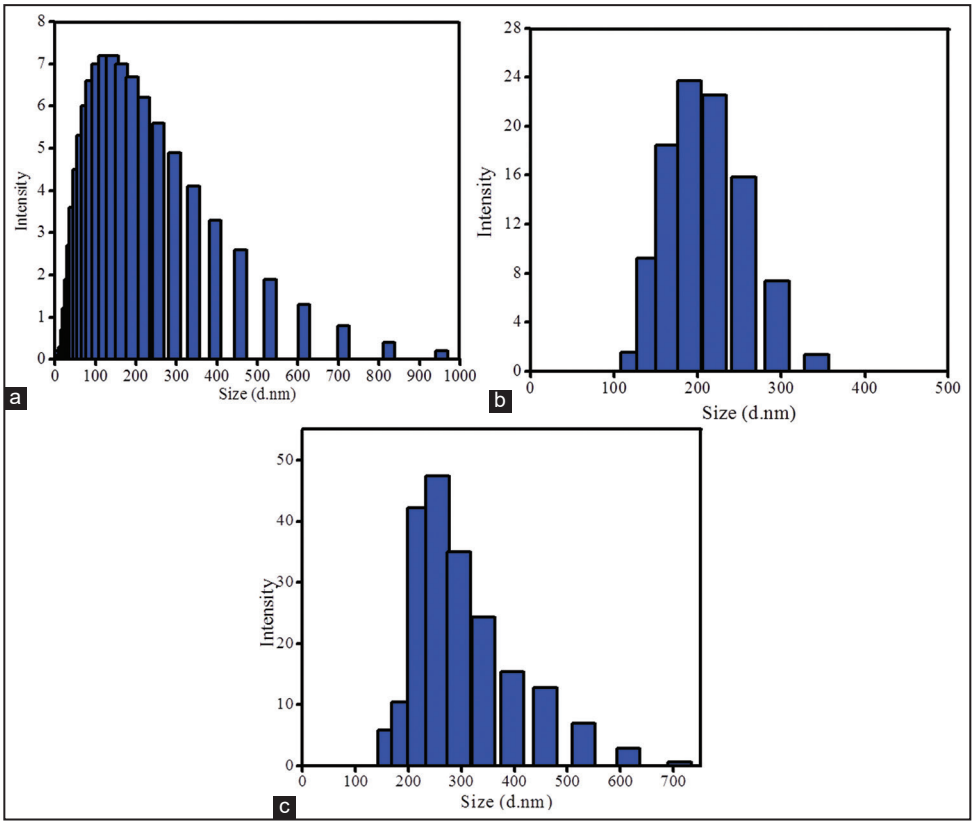

Figure 3: Particle size distribution of (a) PAMNI-2, (b) PAMNI-3, and (c) PAMNI-4 NGs by DLS.

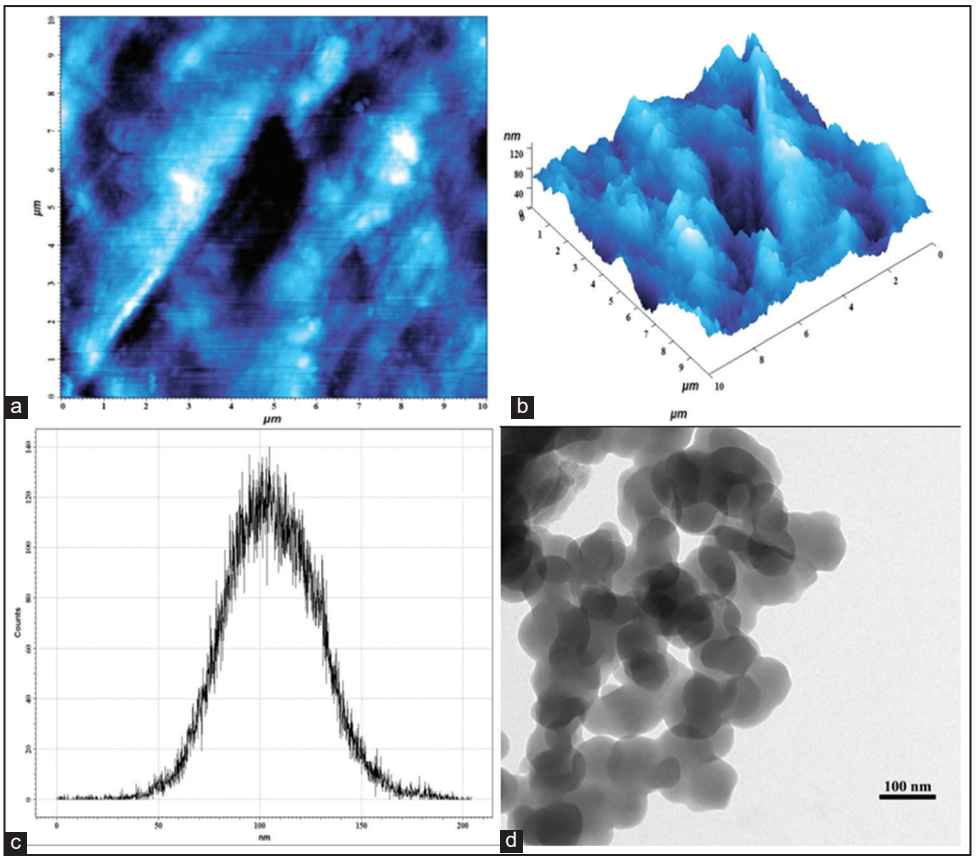

Figure 4: (a) 2-Dimensional, (b) 3-Dimensional morphological images, (c) size distribution of PAMNI-NGs by AFM, and (d) TEM image of PAMNI-NGs.

while the darker spots correspond to less rigid components. From the figure, it could be observed that the individual PAMNI-2-NG particles are fairly circular in shape but the semi-circular spots indicate the agglomeration of NG particles. However, most of the single PAMNI-2-NG particles were found with domain size ranging from 90 to 120 nm [Figure 4c], which shows a good agreement with the results that obtained from DLS studies. TEM is very prompt technique to examine the morphology of PAMNI-2-NGs and the images are displayed in Figure 4d. As extracted from micrographs, it is observed that the PAMNI-2-NGs are semi-spherical in shape and the mean particle size was found as approximately 100 nm, which is significant to that of DLS result.

3.3. XRD Analysis

The dispersion and crystallinity of encapsulated ZDV in the PAMNI-2-NG matrix were investigated from XRD analysis. The X-ray diffractograms of placebo PAMNI-2-NGs, ZDV loaded PAMNI-2-NGs and pristine ZDV are shown in Figure 5. As depicted in the figure, pristine ZDV has shown peaks in between 8 and 38° of 2θ region, while the more intense peak is observed at 2θ of 15° stands for its crystalline behavior. In the case of ZDV-loaded PAMNI-2-NGs, the diffractograms have not shown such intense crystalline peaks which confirmed the presence of ZDV at molecular level dispersion with high homogeneity.

3.4. % Encapsulation Efficiency

The encapsulation efficiency of ZDV in the PAMNI-NGs was evaluated and it was recognized that the values are found in between 33 ± 0.9 and 82 ± 0.8 [Table 1], which hardly depend on the concentration of AMA and MBA. The higher value of %EE (80 ± 1.2) might have resulted for formulation PAMNI-4, have high AMA concentration. The %EE values also found to decrease with increase in MBA concentration

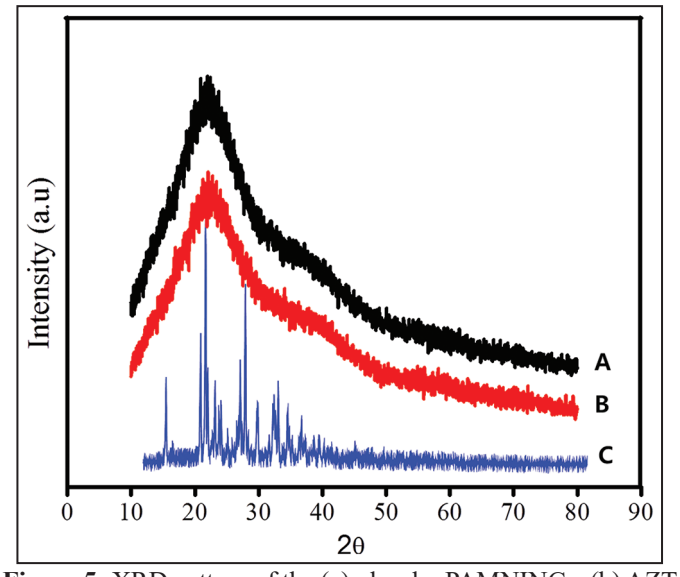

Figure 5: XRD pattern of the (a) placebo PAMNINGs, (b) AZT loaded PAMNI NGs, and (c) pristine AZT.

and the low concentration of MBA is highly favorable to encapsulate maximum drug molecules (82 ± 0.8) into the voids of PAMNI-NGs resulted from less crosslinking points of polymeric chains.

3.5. In Vitro Release Studies

To understand the release behavior of ZDV from PAMNI-NGs, the studies were performed under *in vitro* gastric (pH 1.2) and intestine (pH 7.4) conditions of GIT and were assessed by UV-Vis

spectrophotometer. As shown in Figure 6a and b, the % ZDV release was found to be dependent on pH, monomer (AMA) and crosslinker (MBA) contents, and temperature.

The acidic functionalities of NG networks strongly reflect their pH-responsive behavior. In this connection, the higher release rates of ZDV were found in pH 7.4 rather than pH 1.2, this could be explained by the fact that the NGs showed a higher degree of swelling at pH 7.4 due to ionization of carboxylic groups to carboxylic anions resulted in expansion of the network. In this swollen state, the NGs could release entrapped drug molecules easily through diffusion phenomenon. While the release kinetics at pH 1.2 are less due to shrinking of NG network, wherein, the drug molecules are trapped in the compact network that prevents the leaching of drug molecules. However, at both pH 1.2 conditions, no initial burst release was observed, suggesting that ZDV molecules are effectively protected from the NG network structure.

On the other hand, the *in vitro* release of ZDV was also dependent on AMA content. The % ZDV release from PAMNI-NGs was found to be more as AMA content increased in the network and the results are shown in Figure 7a. The results could be explained from the reason that

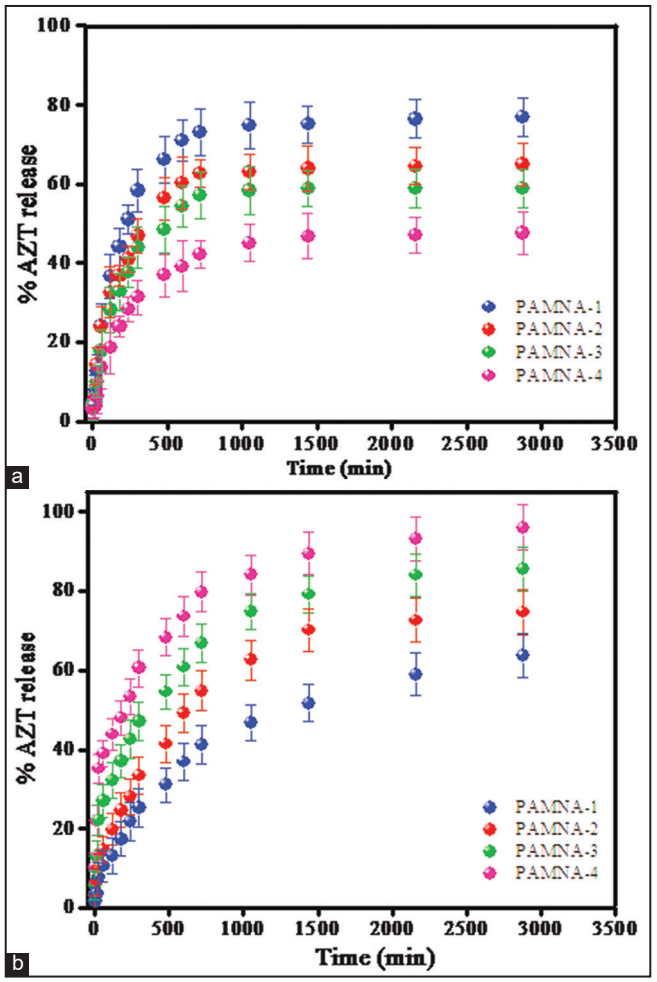

Figure 6: % ZDV release from PAMNI-NGs in (a) pH 1.2 and (b) pH 7.4 (at 37°C).

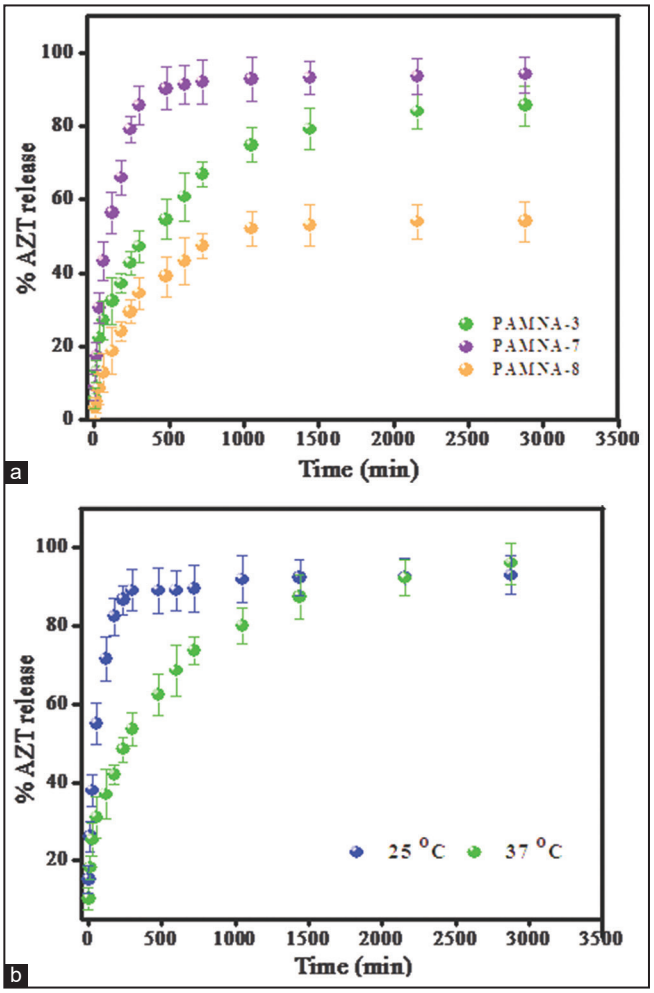

Figure 7: (a) Effect of crosslinker and (b) temperature on % ZDV release from PAMNI-NGs in pH 7.4.

Table 2: Curve fitting results of *in vitro* release data for various kinetic equations.

Sample code	Zero order		First order		Higuchi		Hixson-Crowell		Koresmeyer-Peppas		
	R^2	K_0	R^2	K_1	R^2	K_h	R^2	K_c	R^2	K_p	n
PAMNI-1	0.856	0.094	0.692	0.016	0.962	0.747	0.751	0.028	0.894	0.345	0.729
PAMNI-2	0.936	0.135	0.767	0.015	0.994	0.804	0.834	0.019	0.924	0.233	0.612
PAMNI-3	0.801	0.207	0.631	0.025	0.947	0.356	0.693	0.017	0.774	0.414	1.309
PAMNI-4	0.808	0.491	0.562	0.014	0.971	0.118	0.609	0.016	0.957	0.009	0.422
PAMNI-5	0.933	0.472	0.796	0.015	0.997	0.078	0.857	0.012	0.997	0.065	0.497
PAMNI-6	0.928	0.317	0.98	0.021	0.984	0.025	0.992	0.022	0.914	0.023	0.347
PAMNI-7	0.909	0.395	0.741	0.016	0.986	0.267	0.805	0.013	0.791	0.047	0.437
PAMNI-8	0.972	0.132	0.851	0.012	0.988	1.142	0.901	0.024	0.904	0.049	0.341

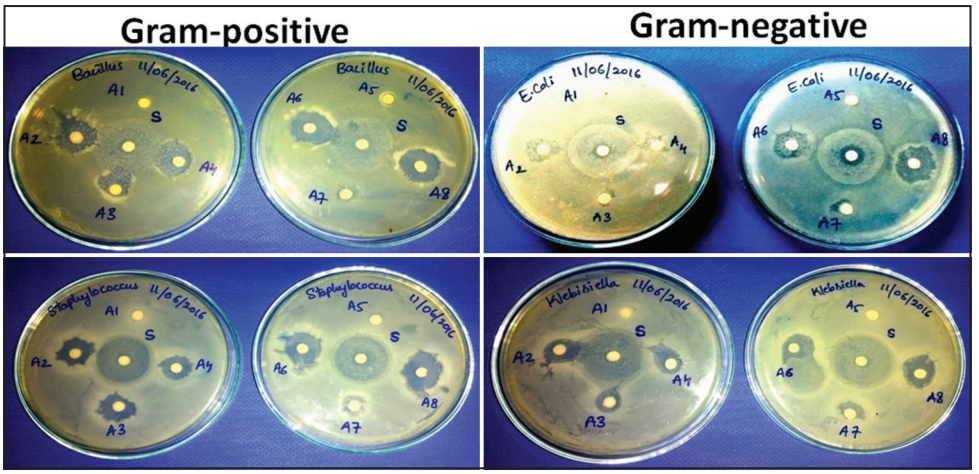

Figure 8: Antibacterial activity images of PAMNI-NGs against Gram-positive (*Bacillus* and *Staphylococcus*), and Gram-negative (*Escherichia coli* and *Klebsiella pneumonia*) bacteria (A1) PAMNI-1, (A2) PAMNI-2, (A3) PAMNI-3, (A4) PAMNI-4, (A5) PAMNI-5, (A6) PAMNI-6, (A7) PAMNI-7, (A8) PAMNI-8, and (s) antibiotic drug.

as more and more AMA is added into the network, large numbers of carboxyl ions are available for the network which results in more ionic repulsions within the structure, and hence more expansion occurred. Therefore, the release of ZDV is more. In the present investigation, PAMNI-4 released 79% of ZDV in a period of 12 h, since it contains a high amount of AMA. In the case of PAMNI-3, 2, and 1, lower release rates were observed, respectively, due to the decrease in the AMA content.

In addition, the drug release behavior also affected by changing the MBA content, since the crosslinking of network plays an important role during the drug release phenomenon. The more compact network has generally resulted from the high amount of MBA, which shows lesser ZDV release, as the rigid network holds the drug molecules more tightly and could not be released out them easily into the medium. In contrast, the lesser crosslinking density of network has the ability to release maximum ZDV. As shown in Figure 7a, PAMNI-7 has less crosslinking density, hence showed initial burst release, that is, 85% in 5 h followed by controlled release due to rapid swelling behavior. While PAMNI-8 exhibited only 34% ZDV release in 5 h. In the case of PAMNI-3, a moderate release behavior was observed, that is, 47% in 5 h.

Besides pH, AMA, and MBA, another important parameter which affects the release behavior of ZDV from PAMNI networks is temperature, since the construction of networks includes thermoresponsive PNIPAM. The effect of temperature on drug release studies was investigated for formulation PAMNI-6, having the maximum amount of NIPAM and the studies were conducted at below (25°C) and above (37°C) LCST point of PNIPAM in pH 7.4. From Figure 7b, it was found that below LCST, the network exhibits a maximum degree of swelling due to relaxation of NIPAM polymeric chains caused by surrounding solvent medium. However, the hydrodynamic diameter of the voids of the matrix was drastically reduced as the temperature increased from 25 to 37°C, indicating volume phase transition of PNIPAM, consequently, and a compact structure was resulted by dehydration of network. From Figure 7b, it could be found that 87% of the initial burst release of ZDV was observed in 4 h, whereas only 47% was released in similar time period. All the above results concluded that the release behavior of ZDV was predominantly dependent on pH, AMA, and MBA as well temperature. The typical pH and temperature sensitivity of NGs would be favorable for controlled drug release studies with excellent encapsulation efficiency.

Table 3: Antibacterial activity data of PAMNI NGs.

Sample Code	Gram-positive		Gram-negative	
	Bacillus cereus	*Staphylococcus aureus*	*Escherichia coli*	*Klebsiella pneumoniae*
	Inhibition zone (mm)+ Paper disc width (mm)			
PAMNI-1	8	7	6	6
PAMNI-2	16	17	14	12
PAMNI-3	14	15	8	8
PAMNI-4	19	12	10	12
PAMNI-5	8	8	7	7
PAMNI-6	22	16	16	14
PAMNI-7	12	7	8	13
PAMNI-8	18	17	17	15
Control	29	22	27	7

By analyzing the *in vitro* release data using different kinetic models, the transport mechanism of ZDV release was depicted. The calculated values are represented in Table 2 and from the results, it is noticed that Higuchi model best describes the release mechanism followed by zero order equation. The higher regression coefficient (R^2) values (>0.947) have been found in the case of Higuchi square root model, which indicates that the release of ZDV from copolymeric NGs is directly proportional to the square root of the time. The exponent *n* values obtained from Koresmeyer-Peppas model are found in between 0.309 and 0.729 explained that the transport of drug follows both Fickian and non-Fickian diffusion phenomena. From kinetic parameters, it was found that the maximum amount of drug (C_{max}) was released in pH 7.4 as compared to pH 1.2 medium. This may be due to the higher swelling behavior of anionic copolymeric PAMNI-NG networks at the alkaline condition.

3.6. Antibacterial Studies

PAMNI-NGs were further screened for the antibacterial assay to investigate the activity of aminothiazole functionality. Four bacterial strains, namely, *B. cereus*, *S. aureus*, *E. coli,* and *K. pneumonia,* were used in the present investigation. The results of zone inhibition are depicted in Figure 8 and Table 3. As from the results, we could know that the maximum activity of PAMNI-NGs was found for Gram-positive

bacteria. Due to excellent chemical stability, tunable particle size, high surface to volume ratio, and enhanced penetrating ability make the NGs easier to interact and to penetrate into the microorganisms. The potential activity of NGs aroused due to the interaction of positively charged carboxylic proton of the copolymeric network with negatively charged phospholipids of the bacterial cell wall. Due to these ionic interactions, the copolymeric PAMNI-NGs easily diffused into the cytoplasmic membrane, where they can bind to the substrates of cell membrane or microorganism to induce cascade effects causing cell lysis [28]. These anti-microbial results and activity mechanism are supported by our laboratory earlier results [29-36].

4. CONCLUSION

In this study, a series of dual-responsive PAMNI copolymeric NGs were successfully developed by a free radical polymerization method. Production of NGs was carried out by varying conditions, the size is found in between 90 and 120 nm. Semi spherical NGs were confirmed from the TEM and AFM studies. Furthermore, PAMNI-NGs were demonstrated for colon delivery of ZDV, an anti-HIV drug. About 33–82% encapsulation of ZDV was achieved for different formulations. *In vitro* release studies of ZDV, encapsulated PAMNI NGs showed that controlled release was observed over a period of 12 h. In addition, the anti-bacterial experiments exhibited profound inhibitory activity against both Gram-positive (*B. cereus* and *S. aureus*) and Gram-negative (*E. coli* and *K. pneumonia*) bacteria. Thus, the PAMNI-NGs can be beneficial for biomedical applications.

5. REFERENCES

1. S. K. Sahoo, S. Parveen, J. J. Panda, (2007) The present and future of nanotechnology in human health care, ***Nanomedicine***, **3:** 20-31.
2. J. K. Oh, D. I. Lee, J. M. Park, (2009) Biopolymer-based microgels/nanogels for drug delivery applications, ***Progress in Polymer Science***, **34:** 1261-1282.
3. H. Zhang, Y. Zhai, J. Wang, G. Zhai, (2016) New progress and prospects: The application of nanogel in drug delivery, ***Materials Science and Engineering: C***, **60:** 60560-568.
4. K. M. Rao, K. S. V. K. Rao, C. S. Ha, (2018) Chapter 6-Functional stimuli-responsive polymeric network nanogels as cargo systems for targeted drug delivery and gene delivery in cancer cells, ***Design of Nanostructures for Theranostics Applications***, **2018:** 243-275.
5. K. M. Rao, K. S. V. Krishna Rao, G. Ramanjaneyulu, C. S. Ha, (2015) Curcumin encapsulated pH sensitive gelatin based interpenetrating polymeric network nanogels for anti-cancer drug delivery, ***International Journal of Pharmaceutics***, **478:** 788-795.
6. S. V. Vinogradov, (2007) Polymeric nanogel formulations of nucleoside analogs, ***Expert Opinion on Drug Delivery***, **4:** 5-17.
7. T. Nochi, Y. Yuki, H. Takahashi, S. I. Sawada, M. Mejima, T. Kohda, N. Harada, I. G. Kong, A. Sato, N. Kataoka, D. Tokuhara, (2010) Nanogel antigenic protein-delivery system for adjuvant-free intranasal vaccines, ***Nature Materials***, **9:** 572-578.
8. R. Sunasee, P. Wattanaarsakit, M. Ahmed, F. B. Lollmahomed, R. Narain, (2012) Biodegradable and nontoxic nanogels as nonviral gene delivery systems, ***Bioconjugate Chemistry***, **23:** 1925-1933.
9. N. Siddiqui, M. F. Arshad, W. Ahsan, M. S. Alam, (2009) Thiazoles: A valuable insight into the recent advances and biological activities, ***International Journal of Pharmaceutical Sciences and Drug Research***, **1:** 136-143.
10. A. Mohammadi-Farani, A. Foroumadi, M.R. Kashani, A. Aliabadi, (2014) N-Phenyl-2-p-tolylthiazole-4-carboxamide derivatives: Synthesis and cytotoxicity evaluation as anticancer agents, ***Iranian Journal of Basic Medical Sciences***, **17:** 502-508.
11. P. Y. Lin, R. S. Hou, H. M. Wang, I. J. Kang, L. C. Chen, (2009) Efficient synthesis of 2-aminothiazoles and fanetizole in liquid PEG-400 at ambient conditions, ***Journal of the Chinese Chemical Society***, **56:** 455-458.
12. F. Mjambili, M. Njoroge, K. Naran, C. De Kock, P. J. Smith, V. Mizrahi, D. Warner, K. Chibale (2014) Synthesis and biological evaluation of 2-aminothiazole derivatives as antimycobacterial and antiplasmodial agents, ***Bioorganic and Medicinal Chemistry Letters***, **24:** 560-564.
13. I. Kayagil, S. Demirayak (2009) Synthesis and anticancer activities of some thiazole derivatives, ***Phosphorus, Sulfur, and Silicon and the Related Elements***, **184:** 2197-2207.
14. A. A. Laila, I. E. Hussein, (2015) DNA binding of ethyl 2-substituted aminothiazole-4-carboxylate analogues: A molecular modeling approach to predict their antitumor activity, ***Future Journal of Pharmaceutical Sciences***, **1:** 1-7.
15. K. S. Hmood, A. N. Elias, (2017) Synthesis, characterization, and antimicrobial evaluation of new ceftriaxone derivatives, ***Iraqi Journal of Pharmaceutical Sciences***, **23:** 75-88.
16. R. Mocelo-Castell, C. Villanueva-Novelo, D. Cáceres-Castillo, R. M. Carballo, R. F. Quijano-Quiñones, M. Quesadas-Rojas, Z. Cantillo-Ciau, R. Cedillo-Rivera, R. E. Moo-Puc, L. M. Moujir, G. J. Mena-Rejón, (2015) 2-Amino-4-arylthiazole derivatives as anti-giardial agents: Synthesis, biological evaluation and QSAR studies, ***Open Chemistry***, **13:** 1127-1136.
17. N. S. Reddy, K. S. V. Krishna Rao, K. M. Rao, S. Parambadath, C. S. Ha, (2016) Aminothiozolyl maleamic acid based multi chelating hydrogels for the separation of uranium (VI) ions from aqueous environment, ***Polymers for Advanced Technologies***, **27:** 1317-1324.
18. Y. Ling, M. Lu, (2008) Preparation and characterization of pH and temperature dual responsive-, Poly (N-isopropylacrylamide-co-itaconic acid) hydrogels using DMF and water as mixed solvents, ***Polymer Journal***, **40:** 592-600.
19. J. Yang, D. D. Hu, H. Zhang (2012) Preparation and thermally induced adhesion properties of a poly (vinyl alcohol)-gN-isopropylacrylamide copolymer membrane, ***Reactive and Functional Polymers***, **72:** 438-445.
20. G. Fundueanu, M. Constantin, P. Ascenzi, (2008) Preparation and characterization of pH-and temperature-sensitive pullulan microspheres for controlled release of drugs, ***Biomaterials***, **29:** 2767-2775.
21. M. Khorram, E. Vasheghani-Farahani, N. G. Ebrahimi, (2003) Fast responsive thermosensitive hydrogels as drug delivery systems, ***Iranian Polymer Journal***, **12:** 315-322.
22. K. M. Rao, B. Mallikarjuna, K. S. V. Krishna Rao, S. Siraj, K. C. Rao, M. C. S. Subha (2013) Novel thermo/pH sensitive nanogels composed from poly (N-vinylcaprolactam) for controlled release of an anticancer drug, ***Colloids and Surfaces B***, **102:** 891-897.
23. M. Shamsipur, S. M. Pourmortazavi, A. A. M. Beigi, R. Heydari, M. Khatibi, (2013) Thermal stability and decomposition kinetic studies of acyclovir and zidovudine drug compounds, ***AAPS PharmSciTech***, **14:** 287-293.
24. E. M. Uronnachi, J. D. Ogbonna, F. C. Kenechukwu, M. A. Momoh, A. A. Attama, V. C. Okore (2013) Pharmacokinetics and biodistribution of zidovudine loaded in a solidified reverse micellar delivery system, ***International Journal of Drug Delivery***, **5:** 73-80.

25. R. C. Doijad, D. S. Bhambere, F. V. Manvi, N. V. Deshmukh, (2009) Formulation and characterization of vesicular drug delivery system for anti-HIV drug, ***Journal of Global Pharma Technology***, **1:** 94-100.
26. S. Panda, S. Pattnaik, L. Maharana, G. B. Botta, A. K. Mahapatra, (2013) Design and evaluation of zidovudine loaded natural biodegradable microcapsules employing colophony resin as microencapsulating agent, ***International Journal of Pharmacy and Pharmaceutical Sciences***, **5:** 799-805.
27. S. Eswaramma, N. S. Reddy, K. S. V. Krishna Rao, (2017) Phosphate crosslinked pectin based dual responsive hydrogel networks and nanocomposites: Development, swelling dynamics and drug release characteristics, ***International Journal of Biological Macromolecules***, **103:** 1162-1172.
28. L. Sun, Y. Du, L. Fan, X. Chen, J. Yang, (2006) Preparation, characterization and antimicrobial activity of quaternized carboxymethyl chitosan and application as pulp-cap, ***Polymer***, **47:** 1796-1804.
29. K. S. V. Krishna Rao, P. R. S. Reddy, Y. I. Lee, C. Kim, (2012) Synthesis and characterization of chitosan-PEG-Ag nanocomposites for antimicrobial application, ***Carbohydrate Polymers***, **87:** 920-925.
30. C. S. Espenti, K. K. Rao, K. M. Rao, (2016) Bio-synthesis and characterization of silver nanoparticles using *Terminalia chebula* leaf extract and evaluation of its antimicrobial potential, ***Materials Letters***, **174:** 129-133.
31. P. R. S. Reddy, S. Eswaramma, K. S. V. Krishna Rao, Y. I. Lee (2014) Dual responsive pectin hydrogels and their silver nanocomposites: Swelling studies, controlled drug delivery and antimicrobial applications, ***Bulletin of the Korean Chemical Society***, **35:** 2391-2399.
32. K. Nagaraja, K. M. Rao, G. V. Reddy, K. S. V. Krishna Rao, (2021) Tragacanth gum-based multifunctional hydrogels and green synthesis of their silver nanocomposites for drug delivery and inactivation of multidrug resistant bacteria, ***International Journal of Biological Macromolecules***, **174:** 502-511.
33. P. R. S. Reddy, K. S. V. Krishna Rao, K. M. Rao, N. S. Reddy, S. Eswaramma, (2015) pH sensitive poly (methyl methacrylate-co-acryloyl phenylalanine) nanogels and their silver nanocomposites for biomedical applications, ***Journal of Drug Delivery Science and Technology***, **29:** 81-188.
34. N. S. Reddy, S. Eswaramma, I. Chung, K. S. V. Krishna Rao, P. Ramesh, A. Chandra Sekhar, (2019) Chitosan/poly (dimethylaminoethylmethacrylate-co-hydroxyethylacrylate) based semi-IPN hydrogels and silver nanocomposites: Synthesis, evaluation of amoxicillin release studies, and antibacterial studies, ***International Journal of Polymeric Materials and Polymeric Biomaterials***, **68:** 870-880.
35. K. Nagaraja, K. S. V. Krishna Rao, S. Zo, S. Soo Han, K. M. Rao, (2021) Synthesis of novel tamarind gum-co-poly (acrylamidoglycolic acid)-based pH responsive semi-IPN hydrogels and their ag nanocomposites for controlled release of chemotherapeutics and inactivation of multi-drug-resistant bacteria. ***Gels***, **7:** 237.
36. S. Vidyasagar Babu, S. Eswaramma, K. S. V. Krishna Rao, (2018) Synthesis, characterization, luminescence and biological activities of lanthanide complexes with a hydrazone ligand, ***Main Group Chemistry***, **17:** 99-110.